Observation and modeling of α-NiPtAl and Kirkendall void formations during interdiffusion of a Pt coating with a γ-(Ni-13Al) alloy at high temperature

Pauline Audigié, Aurélie Vande Put, André Malié, Pascal Bilhé, Sarah Hamadi, Daniel Monceau

Observation and modeling of α-NiPtAl and Kirkendall void formations during interdiffusion of a Pt coating with a γ-(Ni-13Al) alloy at high temperature

Pauline Audigié [a,*], Aurélie Rouaix-Vande Put [a], André Malié [b], P æc d B ł hé [c], Sarah Hamadi [c], D an èl M œ n œ au [a]

[a] CIRIMAT, University of Toulouse, ENSIACET, 4 Allée Emile Monso, BP 44362, 31030 Toulouse Cedex 4, France
[b] SNECMA, SAFRAN-Group, 99 rue Maryse Bastié, BP 129, 86101 Châtellerault Cedex, France
[c] SNECMA, SAFRAN-Group, rue Henry-Auguste Desbruères, 91003 Evry Cedex, France

A B S T R A C T

During the last 15 years, Pt-rich γ–γ′ bond-coatings have been studied extensively for their corrosion and oxidation resistance, and as a lower cost alternative to β-(Ni,Pt)Al bond-coatings in thermal barrier coating systems. To optimize their fabrication and durability, it is essential to investigate their interdiffusion with Ni-based superalloys. This study reports on experimental results and modeling of the interdiffusion of the model Pt/γ-(Ni-13Al) alloy system. Pt coatings were deposited either by electroplating or by spark plasma sintering using a Pt foil. Heat treatments at 1100 °C for 15 min to 10 h were performed either in a high-temperature X-ray diffraction device under primary vacuum or in a furnace under argon secondary vacuum. The α-NiPtAl phase with $L1_0$ crystal structure formed very rapidly, implying fast uphill Al diffusion toward the surface. For Pt electroplating, α-phase transformed to γ′-$(Ni,Pt)_3Al$ after only 45 min–1 h at 1100 °C. The resulting two-phased γ–γ′ microstructure remained up to 10 h. When using a Pt foil coating, the continuous layer of α-NiPtAl phase disappeared after 10 h and the γ′-$(Ni,Pt)_3Al$ or γ-(Ni,Pt,Al) phase appeared, resulting in two different diffusion paths in the Ni–Pt–Al phase diagram. Voids also formed at the interdiffusion zone/substrate interface for both systems after 1 h or more. Composition analyses confirmed that voids were located at the Pt diffusion front corresponding to the Al-depleted zone. Experiments performed with the samples coated with a Pt foil confirmed that voids are due to a Kirkendall effect and not to the Pt deposition process. Numerical simulations including the cross-term diffusion coefficients in the diffusion flux equations reproduced the experimental concentration profiles for the γ-phased systems.

1. Introduction

Thermal barrier coating systems (TBCs) are widely used to decrease the operating temperature of the Ni-based superalloys in gas turbines [1]. Ni-based superalloys are used because of their mechanical properties at high temperature. To protect against high-temperature oxidation and hot corrosion, Ni-based superalloys are coated with an α-alumina-forming protective coating. β-(Ni,Pt)Al and MCrAlYs are the most commonly used bond-coatings. However, in the last 15 years, the Pt-rich γ–γ′ bond-coatings have been studied for their corrosion and oxidation resistance, and as a lower cost alternative to β-(Ni,Pt)Al bond-coatings in TBC systems [2–4]. Pt-rich γ–γ′ bond-coatings can be superior to β-(Ni,Pt)Al bond-coatings despite a lower initial Al reservoir and a higher sensitivity to the substrate composition [5–7]. Indeed, it has been shown that they decrease rumpling [8–10] and limit or suppress the precipitation of brittle, topologically close-packed (TCP) phases [8,11] resulting from the interdiffusion between the bond-coating and the substrate. Similarly to β-(Ni,Pt)Al, Pt additions improve the oxide scale adherence by reducing the sulfur detrimental effect [12,13]. However, the Pt effect on the coating microstructure is not well understood, especially during the fabrication process. After having published the Ni–Pt–Al phase diagram at 1100 °C [3], Hayashi et al. [14] studied the only ternary phase, named α-NiPtAl, and the associated equilibria at 1150 °C. Monceau et al. [15] showed that α-NiPtAl phase coatings can be seen as precursors of Pt-rich γ–γ′ coatings. But only limited data about this α-phase are available in the literature [16,17].

Voids have also been observed at the bond-coating/substrate interface [18–21]. Vialas and Monceau [19] and Haynes et al. [22] attributed their formation to a Kirkendall effect, but without clear proof. Yamaguchi et al. [20] suggested that cyclic oxidation is an additional source for vacancy supersaturation. Stacy et al. [23] considered that hydrogen dissolution in the material during the Pt electroplating process could be a cause of void formation. In order to improve the TBC lifetime,

* Corresponding author. Tel.: +33 534323448; fax: +33 534323399.
E-mail address: pauline.audigie@ensiacet.fr (P. Audigié).

http://dx.doi.org/10.1016/j.surfcoat.2014.08.083

it is thus important to better understand the diffusion processes during the fabrication of the Pt-rich γ–γ′ bond-coatings, the formation of voids and the long-term evolution of the system, to accurately predict lifetime.

The present study was focused on the interdiffusion behavior of Pt coatings on a γ-(Ni-13Al) substrate in order to follow phase transformations and to determine diffusion paths. Two Pt deposition processes were used to understand if void formation is a processing issue or due to the Kirkendall effect. Pt was deposited on the model alloy either by electroplating or by spark plasma sintering (SPS) using a Pt foil. A computer model based on a previous one developed in the 90's for kinetic demixing in oxides [24] was used and simulations were run to predict the composition profile evolution.

2. Experimental

A polycrystalline alloy rod of Ni-13Al (at.%) was prepared by argon arc melting from high-purity Ni and Al at the Institut Jean Lamour, Nancy (France), and was subsequently annealed for 1 h at 1100 °C in air. After heat treatment, the alloy average grain size was 250 μm. The as-cast alloy mean composition was Ni-13.1Al (at.%), according to energy dispersive spectroscopy analysis with real standards. Samples of 17 mm diameter and 1.5–2 mm thickness were cut and polished with SiC paper down to P600 and cleaned with ethanol in an ultrasonic bath, followed by grit-blasting with α-Al_2O_3 particles. A pure Pt coating, 5 μm thick, was deposited on the substrate by electroplating using the facilities of the SNECMA-SAFRAN Group. Then, heat treatments of 15 min up to 10 h at 1100 °C were performed in a high-temperature X-ray diffraction (HT-XRD) device (BRUKER D8) under primary vacuum, allowing us to follow phase transformations. Lattice parameters were determined from the three main peaks of each phase to be (001), (110) and (111) for α-NiPtAl phase, (111), (200) and (220) for γ-(Ni,Pt,Al) and γ′-$(Ni,Pt)_3Al$ phases.

In order to compare with another Pt deposition process, some samples of Ni-13Al were coated with a 5 μm Pt foil using SPS at a heating rate of 100 °C/min up to 1000 °C followed by a dwell time of 10 min. Uniaxial pressure of 23 MPa was applied from the first minute of the cycle. More details on SPS procedure can be found in [15]. After SPS, samples were heat-treated for 5 min to 10 h at 1100 °C in argon secondary vacuum with rapid heating and cooling (~500 °C/min initial rate). XRD analyses were performed at room temperature after heat treatments.

For both Pt coatings (electroplated and foil-clad), all the resulting interdiffusion zones were cross-sectionally prepared and analyzed by scanning electron microscopy (SEM) and energy dispersive spectroscopy (EDS) using real standards. Electron-probe microanalysis (EPMA) was also performed to determine quantitative Ni, Al and Pt concentration profiles. A computer program using an explicit finite difference (FD) scheme was used to calculate the fluxes and the concentration profiles in the γ system. The fluxes were written as generalized Fick's laws with cross-term diffusion coefficients.

3. Results

3.1. Interdiffusion of electroplated Pt with γ-(Ni-13Al) alloy at 1100 °C

Fig. 1 compares X-ray diffraction patterns for Pt-electroplated Ni-13Al annealed 15 min and 1 h at 1100 °C in the HT-XRD device under primary vacuum. The primary vacuum did not prevent oxidation so α-Al_2O_3 formed on the surface. After 15 min, XRD analyses revealed that the Pt from the coating did not diffuse entirely into the matrix and that α-NiPtAl formed. The lattice parameters of the tetragonal α-phase were found to be $a = 0.386$ nm and $c = 0.353$ nm at room temperature. A heat treatment composed of a fast heating (40 °C/min) and a 100 s dwell at 1100 °C also resulted in the formation of α-NiPtAl with lattice parameters $a = 0.397$ nm and $c = 0.354$ nm after cooling to room temperature. After 15 min at 1100 °C, γ peaks were also observed with a

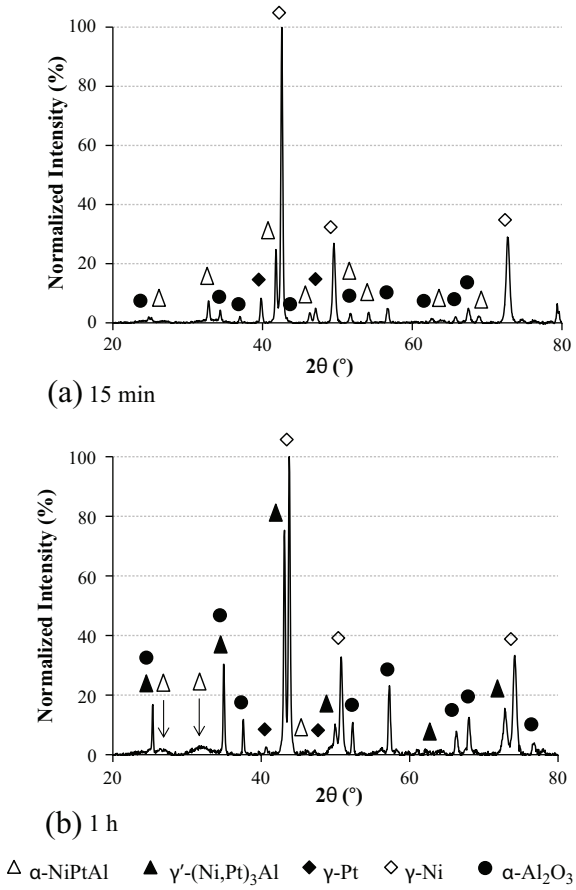

Fig. 1. X-ray diffraction patterns of Pt-electroplated Ni-13Al after (a) 15 min and (b) 1 h at 1100 °C in the HT-XRD device under primary vacuum.

lattice parameter of 0.368 nm, which lies between the cell parameter of Pt (0.392 nm) and that of γ-(Ni-13Al) (0.354 nm). These γ peaks were attributed to the phase present in the interdiffusion zone. For longer annealing times, HT-XRD analyses showed that the α-NiPtAl vanished after 45 min to 1 h. After 1 h, the γ′-$(Ni,Pt)_3Al$ phase appeared with a lattice parameter equal to 0.363 nm. γ peaks were also observed, corresponding to a lattice parameter of 0.359 nm. A two-phased γ–γ′ microstructure was obtained and no significant evolution was seen between 2.5 h and 10 h.

Cross-sections of annealed samples were analyzed by SEM, EDS and EPMA. The microstructure of the systems after 15 min, 1 h, 2.5 h and 10 h at 1100 °C is shown in Fig. 2. The surface undulations correspond to the "cauliflower"-shaped Pt grains obtained after electroplating. α-Al_2O_3 particles from the grit-blasting process mark the initial interface between the Pt coating and the γ alloy. Fig. 2(a) is a cross-section of the interdiffused sample after 15 min. The microstructure can be divided into three zones: the Pt-enriched zone above the initial surface, the interdiffusion zone and the base material. The total thickness of the coating was 17 μm. The Pt-enriched zone, about 6 μm thick, was a mixture of small α-NiPtAl precipitates (brightest phase) in a γ phase matrix. The interdiffusion zone was γ-single-phased with thickness about 11 μm. The Pt diffusion in the substrate was homogeneous with a planar diffusion front. After 1 h at 1100 °C (Fig. 2(b)), the α-NiPtAl phase vanished as confirmed by the XRD analyses (Fig. 1). The brightest phase was γ′-$(Ni,Pt)_3Al$. A two-phased γ–γ′ microstructure resulted. The interdiffusion zone thickness increased with annealing time up to ~25 μm after 10 h (Fig. 2(d)). No phase transformation and no significant microstructural evolution were noticed between 2.5 and 10 h. Moreover, voids were observed at the interdiffusion zone/substrate

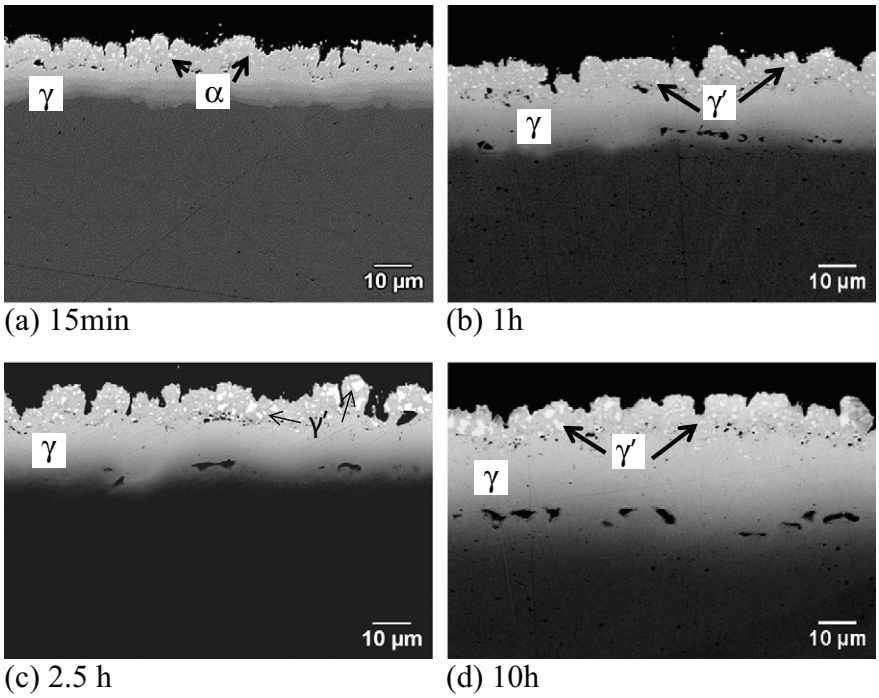

Fig. 2. Backscattered electron images of cross-sections of Pt-electroplated Ni-13Al after (a) 15 min, (b) 1 h, (c) 2.5 h and (d) 10 h at 1100 °C in the HT-XRD device under primary vacuum.

interface after 1 to 10 h, whose number and size increased with time. Concentration profiles and EDS maps confirmed that voids were located at the Pt diffusion front, which also corresponds to the Al-depleted zone.

3.2. Interdiffusion of Pt foil with γ-(Ni-13Al) alloy at 1100 °C

A 5 μm thick Pt foil was deposited on the γ-(Ni-13Al) alloy by SPS to check if void formation is due to electroplating. Fig. 3 compares X-ray diffraction patterns for the Ni-13Al + Pt foil after 5 min and 10 h at 1100 °C under Ar secondary vacuum. As already observed just after SPS fabrication, XRD analyses revealed that all the Pt from the foil reacted with the matrix to form an α-NiPtAl continuous layer after 5 min at 1100 °C. This phase was characterized by $a = 0.388$ nm and $c = 0.352$ nm at room temperature. A graphite peak remained due to the SPS processing [15]. A longer heat treatment was performed for 10 h with XRD revealing α-Al_2O_3 formation caused by the Ar secondary vacuum not preventing oxidation. XRD patterns also revealed the presence of the γ′-$(Ni,Pt)_3Al$ phase and the γ phase of the interdiffusion layer.

Following the same procedure, cross-sections of annealed samples were analyzed by SEM and EDS. The microstructure of the systems after 5 min, 1 h and 10 h at 1100 °C is shown in Fig. 4. When using the SPS process with a Pt foil, the surface roughness was smoother and the coating more uniform than for those done by Pt electroplating. Fig. 4(a) is a cross-section of the interdiffused sample after a rapid heating up to 1100 °C and a dwell time of 5 min. Three zones can be distinguished from the surface. On top, a continuous α-NiPtAl phase ~ 4.8 μm thick was formed whose average composition was determined by EDS to be 39Ni-24Al-37Pt (at.%). Next, a γ interdiffusion zone was observed with a thickness of ~11 μm. Third, the base material was observed. The Pt diffusion front was planar after 10 h (Fig. 4(d)). Furthermore, the microstructure was not homogeneous. In some areas, the layer of the α-NiPtAl phase was replaced by a 5 μm thick layer of γ′-$(Ni,Pt)_3Al$ phase. In other areas, no α or γ′ phase was seen (Fig. 4(c) and (d)). Only a Pt-rich γ phase layer 28 μm thick was observed with concentration gradients of Ni, Al and Pt. Most importantly, voids were observed at the interdiffusion zone/substrate interface after 1 to 10 h. Smaller voids were also seen 5 μm in from the surface, which can be attributed to the processing when the Pt foil is placed over the substrate before SPS. However, cavities at the interdiffusion zone/substrate interface were bigger and looked similar to the ones obtained with Pt electroplating. They were numerous with spherical

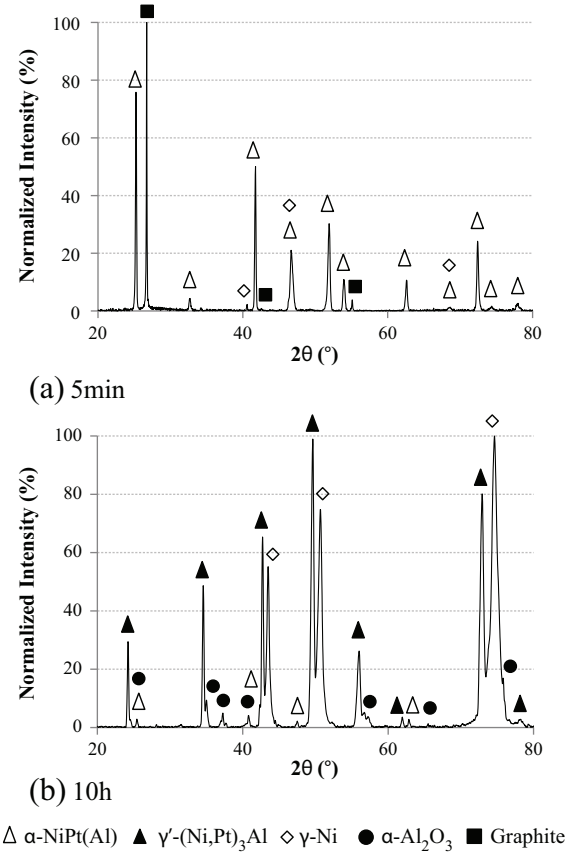

Fig. 3. X-ray diffraction patterns of Ni-13Al + Pt foil after (a) 5 min and (b) 10 h at 1100 °C under Ar secondary vacuum.

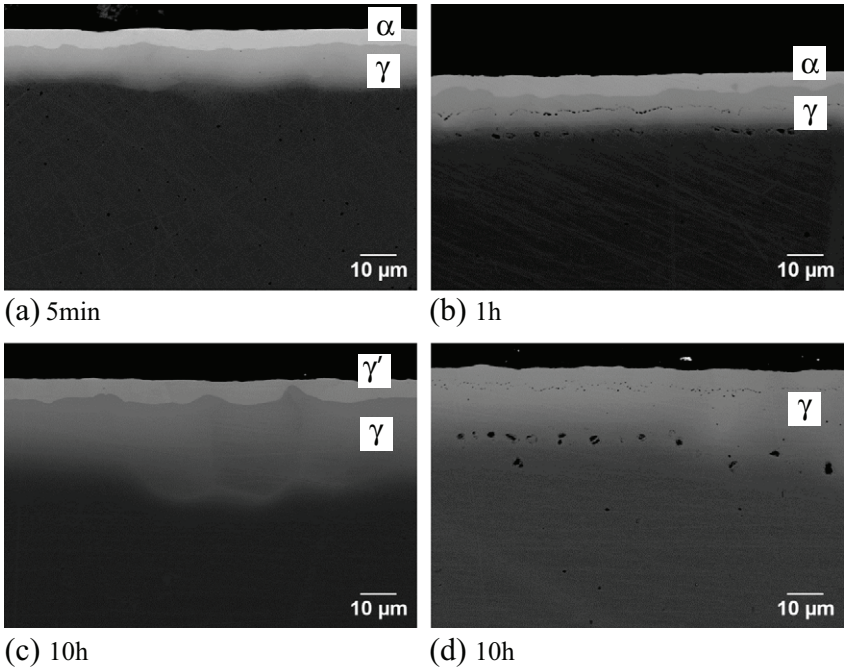

Fig. 4. Backscattered electron images of cross-sections of Ni-13Al + Pt foil after (a) 5 min, (b) 1 h, (c) and (d) 10 h at 1100 °C under Ar secondary vacuum.

morphology. The EPMA concentration profiles in Fig. 5 confirm that voids were located at the Pt diffusion front that also corresponds to the Al-depleted zone.

3.3. Modeling of concentration profiles

Computer simulations were used to calculate the composition profile evolution as well as to predict possible nucleation of new phases. The calculations were done using a one-dimensional finite difference scheme (1D-FD). The calculation domain was a sample of finite size with the hypothesis that the oxidation at the surface could be neglected due to the small oxide-scale thickness compared to the diffusion length in the alloy. The experimental concentration profile after the first process annealing was taken as the initial condition. The local diffusion fluxes of Al and Pt, J_{Al} and J_{Pt}, respectively, were described by Eqs. (1) and (2), and the Ni flux, J_{Ni}, was calculated as the difference (Eq. (3)). $D^{Ni}_{Al\text{ - }Al}$ and $D^{Ni}_{Pt\text{ - }Pt}$ are the main-term interdiffusion coefficients and $D^{Ni}_{Al\text{ - }Pt}$ and $D^{Ni}_{Pt\text{ - }Al}$ are the cross-term interdiffusion coefficients, respectively. $\partial C_{Al}/\partial x$ and $\partial C_{Pt}/\partial x$ are the local concentration gradients of Al and Pt, respectively, and x is the distance from the surface. The diffusion

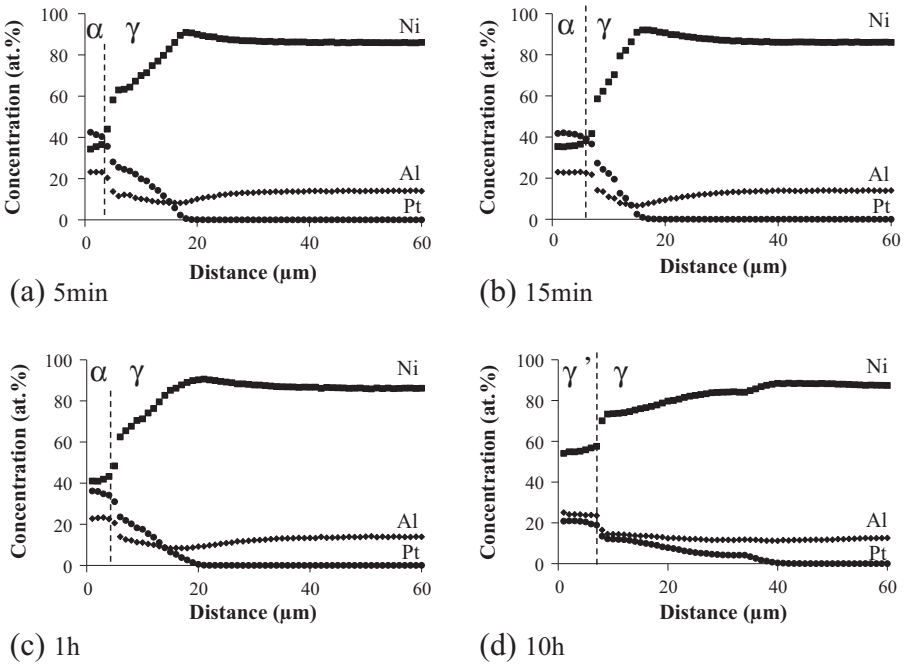

Fig. 5. EPMA concentration profiles for Ni-13Al + Pt foil at 1100 °C after (a) 5 min, (b) 15 min, (c) 1 h and (d) 10 h under Ar secondary vacuum.

Table 1
Diffusion matrix (m^2/s) at 1150 °C [26] used for the FD modeling presented in Fig. 6.

(m^2/s)	Al	Pt
Al	5.5×10^{-14}	-2.5×10^{-14}
Pt	-5.4×10^{-15}	1.2×10^{-14}

process was calculated in the γ phase. Because oxidation was neglected and diffusion in the multi-phased material was not considered, the calculations were performed without any moving phase boundaries.

$$J_{Al} = -D^{Ni}_{Al\text{-}Al}\partial C_{Al}/\partial x - D^{Ni}_{Al\text{-}Pt}\partial C_{Pt}/\partial x \quad (1)$$

$$J_{Pt} = -D^{Ni}_{Pt\text{-}Pt}\partial C_{Pt}/\partial x - D^{Ni}_{Pt\text{-}Al}\partial C_{Al}/\partial x \quad (2)$$

$$J_{Ni} = -J_{Al} - J_{Pt} \quad (3)$$

Before simulating our experiments, the first step was to verify the model accuracy. In that respect, comparisons were done with literature data. First, simulations were compared with the Sundman et al. [25] results for a Ni-5Al (at.%) alloy coated with 2 μm of electroplated Pt. These authors calculated the diffusion profiles in the single-phased system, using the "diffusion-controlled transformations software" (DICTRA) using thermodynamic and mobility data. The Ni, Al and Pt composition profiles after 1 h at 900 °C were used as the initial conditions to limit the rapid initial Pt diffusion which was attributed by the authors to the nano-crystallized microstructure of the Pt electroplated coating. Simulations were run up to 11 h at 900 °C. Second, our simulations were compared with Hayashi et al. [26] obtained at 1150 °C for the γ-diffusion couple Ni-14Al-10Pt/Ni-7Al-18Pt (at.%). The numerical simulations of these authors used the numerical NASA software "Coating Oxidation and Substrate Interdiffusion Model" (COSIM). Hayashi et al. determined the interdiffusion coefficients by applying the analytical method from Kirkaldy, an extension to ternary systems of the Boltzmann-Matano method. The diffusion matrix used is recalled in Table 1. Fig. 6 compares the DICTRA or COSIM results with our FD calculations. Good agreement was found for both tests in spite of slight discrepancies in the interdiffusion zone for the γ-diffusion couple.

Having validated our model, we could apply our simulation tool to our experimental results. Fig. 7 compares experimental and calculated profiles for Pt-electroplated Ni-13Al after 1 h and 10 h at 1100 °C under primary vacuum. The Ni, Al and Pt composition profiles after 15 min at 1100 °C were considered as the initial conditions. Experimental and calculated profiles were found to be in reasonable agreement for the γ-phased systems and the expected Al uphill diffusion was predicted by the model. The fitted interdiffusion coefficients at 1100 °C were in the range of those in the literature and are gathered in Table 2. As reported, the main-term matrix coefficients are positive and $D^{Ni}_{Al\text{-}Al}$ is higher than $D^{Ni}_{Pt\text{-}Pt}$ by an order of magnitude. The cross-term matrix coefficients are negative and within the same order of magnitude as the main-term coefficients.

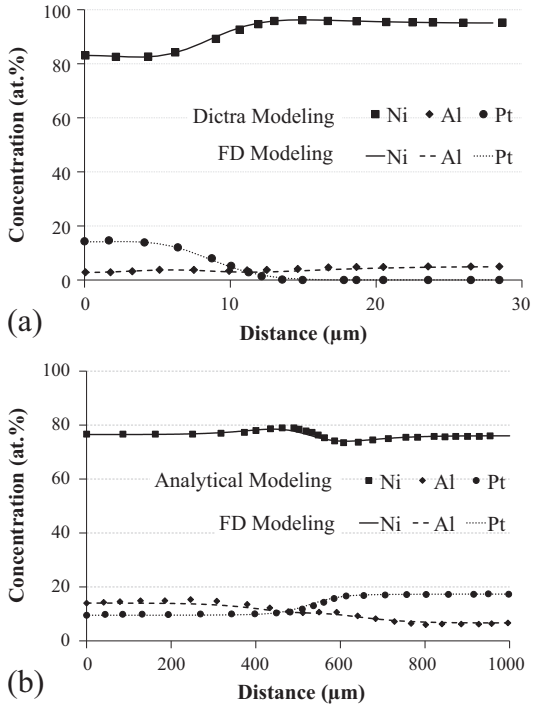

Fig. 6. Simulation testing of the FD model using literature data: (a) comparison of DICTRA [25] and FD model for Ni-5Al (at.%)/2 μm Pt after 11 h at 900 °C, (b) comparison of analytical method [26] and FD model for the γ diffusion couple (Ni-14Al-10Pt/Ni-7Al-18Pt) after 50 h at 1150 °C.

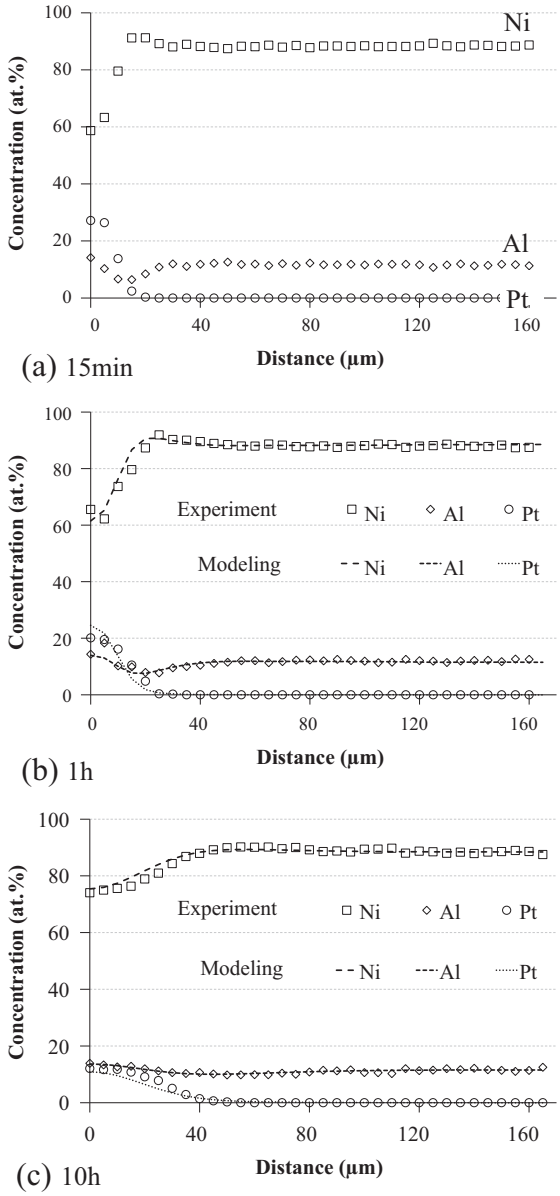

Fig. 7. (a) Initial profiles used for modeling (15 min at 1100 °C) and comparison of calculated (solid lines) and experimental (open symbols) profiles for Pt-electroplated Ni-13Al after (b) 1 h, and (c) 10 h, at 1100 °C under primary vacuum.

Table 2
Diffusion matrix (m^2/s) at 1100 °C used for experimental results, presented in Fig. 7.

m^2/s	Al	Pt
Al	2.9×10^{-15}	-1.2×10^{-15}
Pt	-4.6×10^{-16}	6.8×10^{-16}

4. Discussion

4.1. α-NiPtAl formation and diffusion paths

After heat treatment at 1100 °C under Ar secondary vacuum, the Pt layer deposited on a γ-(Ni-13Al) substrate led to the formation of the α-NiPtAl phase with the $L1_0$ crystal structure. The α-NiPtAl phase formation can be related to Gleeson et al. [3] showing that platinum decreases the Al activity, which promotes the Al uphill diffusion from the alloy to the surface [3,27]. But the intensity of this uphill diffusion leading to the α-NiPtAl phase formation from two γ phases containing initially 0 and 13 at.% Al can be impressive. From the modeling results, since Al and Pt concentration gradients were of opposite sign; the negative value of the cross-term coefficient $D^{Ni}_{Pt\ -\ Pt}$ suggests that Al flux is increased by the presence of Pt in the top layer. This is consistent with the fact that Pt decreases the chemical activity of Al. As a consequence, Al diffuses faster toward the surface with Pt than without Pt. Al even diffuses uphill when its concentration in the surface layer is higher than that in the bulk.

In the present study which made use of "Pt-only" coatings, all the Al present in the α-phase comes from the γ-substrate containing 13 at.% of Al. Al diffuses toward the surface to finally form α-NiPtAl containing about 24 at.% of Al, i.e., much more than in the substrate. An Al depletion zone was observed deeper in the sample corresponding to the Pt diffusion front. The presence of a Pt layer on a commercial superalloy can change the Al concentration from 12 at.% to at least 23 at.% and lead to the γ′-phase formation. Bouhanek et al. [2] were among the first to observe the γ′ phase obtained after Pt deposition and annealing, a precursor of many other studies showing that Pt-rich γ–γ′ bond-coatings can be obtained without any Al external source [18,21,22]. For a Pt-modified NiCoCrAlYTa coating, Vande Put et al. [28] also remarked that the Pt effect on the Al activity was so extensive that it resulted in the formation of martensitic β-(Ni,Pt)Al, with about 37 at.% of Al.

Regarding α-NiPtAl formation, the Ni–Pt–Al phase diagrams reported in Figs. 8 and 9 show that its domain exists over a wide and still unknown composition range. Kamm and Milligan [16] reported the α-NiPtAl formation in their phase equilibria study of Pt-rich Ni-Al-Pt alloys at 1100 °C, followed by Meininger and Ellner [17] after interdiffusion at 1100 °C of the Ni_3Al/Pt_3Al diffusion couple. Hayashi et al. [14] completed these results showing that the α-NiPtAl phase can be formed in a Ni/Pt_3Al couple after a heat treatment for 50 h at 1150 °C. Saint Ramond et al. [29] showed that α phase can be an alternative bond-coating in TBC systems.

Thus, protective coatings could be obtained on a gas turbine part either by Pt electroplating followed by a vapor-phase aluminizing step or by sequential sputtering Al and Pt layers. Two years later, the fabrication of Pt-rich γ–γ′ coatings by using Pt and Al stacking foils of different thicknesses, using a SPS process, was published [10,15]. These authors showed that α-NiPtAl coatings can be seen as precursors of Pt-rich γ–γ′ coatings. Nevertheless, γ–γ′ coatings can be obtained also after the formation of β-(Ni,Pt)Al, depending on the targeted γ–γ′ coating composition and on the Al and Pt initial quantities, since both diffusion paths are possible [15].

As shown in Fig. 4(a), the α-phase thickness after 5 min at 1100 °C was 4.8 ± 0.6 μm whereas the Pt foil was 5 μm thick. This suggests that the Pt flux out of the foil was balanced by the sum of Ni and Al fluxes toward the surface. This results in the formation of a surface γ-(Ni,Pt,Al) layer, where α phase precipitates when the Ni and Al concentrations became large enough. This α phase vanishes after 45 min–1 h at 1100 °C, when Pt continues to diffuse toward the bulk,

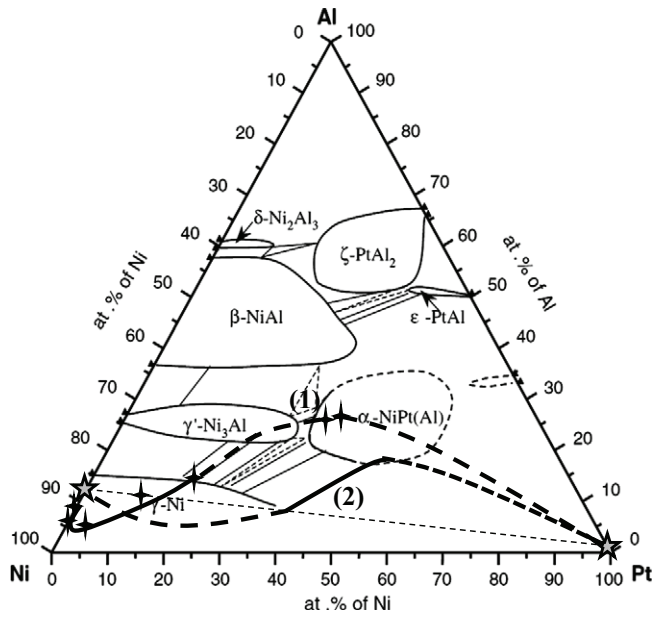

Fig. 8. Diffusion path of Ni-13Al + Pt foil after 15 min at 1100 °C under Ar secondary vacuum, on the Ni–Pt–Al diagram of Hayashi et al. [14]. Crosses correspond to experimental values. Continuous lines are known paths and dashed lines are speculated paths.

and Al diffuses back to the bulk when the γ′-$(Ni,Pt)_3Al$ phase or the γ-(Ni,Pt,Al) phase appears. According to the Ni–Pt–Al phase diagram, two diffusion paths are possible (Fig. 8):

(1) Pt–α-NiPtAl–γ′-$(Ni,Pt)_3Al$–γ-(Ni,Pt,Al)–Ni-13Al
(2) Pt–α-NiPtAl–γ-(Ni,Pt,Al)–Ni-13Al.

The first one was deduced from the observations in Fig. 8 for Ni-13Al + Pt foil after 15 min at 1100 °C under Ar secondary vacuum. This first diffusion path corresponds to the following sequence of phases observed in the surface layer:

Pt ➔ α-NiPtAl ➔ γ′-$(Ni,Pt)_3Al$ + γ-(Ni,Pt,Al)

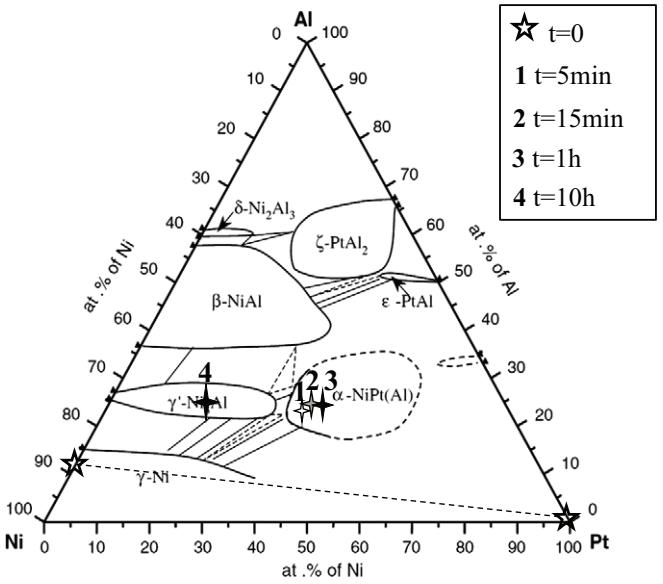

Fig. 9. Evolution of the surface concentration with time for Ni-13Al + Pt foil annealed at 1100 °C under Ar secondary vacuum, displayed on the Ni–Pt–Al diagram from Hayashi et al. [14].

As mentioned previously, after 10 h at 1100 °C, the microstructure of Ni-13Al + Pt foil was not homogeneous and, in some areas, a γ′-$(Ni,Pt)_3Al$ sub-surface zone was observed. Fig. 9 presents the evolution of the surface concentration of the Ni-13Al + Pt foil. This confirms that α-NiPtAl formed very quickly and that no significant compositional evolution was observed between 5 min and 1 h. After 10 h, only Ni and Pt concentrations evolved; the Al concentration staying constant at 25 at.%. This highlights that α ➔ γ′ transformation occurs by Pt–Ni substitution. To model fully the appearance and disappearance of the α phase, more work is needed in order to determine the diffusion data in the α phase. If the α phase is considered as a coating, its mechanical properties will have to be determined.

4.2. Kirkendall voids

In the present work, for both studied systems, a Pt electroplating or a Pt foil deposited on a γ-(Ni-13Al) substrate, a large number of voids formed after 1 h at 1100 °C, located at the interdiffusion zone/substrate interface. Void location also corresponded to the Pt diffusion front and to the Al depletion zone, which disrupted the coating/substrate microstructure. The formation of such voids was observed by Purvis and Warnes [30], the first to highlight Kirkendall porosity in Pt-plated pure Ni after 2–6 h at 950 °C and 1080 °C. Voids were located at the Pt coating/Ni 200 alloy interface. These authors justified void formation as being a result of faster diffusion of Ni than Pt. Susan and Marder [31] observed porosities at the coating/superalloy interface after 1000 h of interdiffusion at 1000 °C of a Ni-matrix/Al-particle composite coating with a nickel substrate, explained as the result of the Kirkendall effect during Al diffusion to the substrate.

In 2006, Vialas and Monceau [19] presented numerous voids in a β-(Ni,Pt)Al coating/single crystal "B" (SCB) superalloy system after very long-term oxidation tests. The aluminization of the sample was defective and the coating was Al-poor. Indeed, after 1800 h at 1050 °C, the coating microstructure was Pt-rich γ–γ′. Voids formed at the metal/oxide interface, typical for β-coatings, but also deeper in the substrate, in particular at the γ′/SCB superalloy interface, where they were observed in large quantities after 10,500 h at 1050 °C. Interestingly, voids were not observed in the same conditions with a non-defective β-(Ni,Pt)Al coating. The authors suggested a Kirkendall effect to explain void formation, but without justification.

The Oak Ridge group has long studied the interdiffusion and oxidation behavior of a Pt-rich γ–γ′ bond-coating obtained by Pt electroplating on a Ni-based superalloy [4,18,21,23,32]. After fabrication, the authors also remarked on voids at the γ′/superalloy interface, whose size and proportion seemed to depend on the electroplating conditions, such as the hydrogen evolution [23]. The void size and number increased after diffusion during 1000 h at 1000 °C or 1050 °C.

In 2009, Haynes et al. [22] observed many cavities after 1000 1 h-cycles at 1150 °C for a Pt-rich γ–γ′/Y-containing N5 system, whereas after 2400 cycles at the same temperature the β-(Ni,Pt)Al/Y-containing N5 system exhibited many fewer voids. The authors suggested that the voids came from the Al loss due to its uphill diffusion toward the surface implying that the Al flux would not be fully compensated by the other fluxes toward the superalloy.

Hayashi et al. [14] have also studied the Ni–Pt–Al ternary system. They showed a significant amount of porosity and cracking in the interdiffusion zone in a Ni_3Al/Pt_3Al couple after 50 h at 1150 °C. But no evidence of voids was shown for γ/γ or γ′/γ′ couples of different compositions [26]. There was also no evidence of void formation within the Pt-rich γ–γ′ bond-coating on the AM1 superalloy after fabrication by SPS from Pt foils, or Pt and Al foil stacking [10,15,33]. This last observation could be due to sintering under pressure. However, Selezneff [34] observed three cavities at the γ′/superalloy interface in a SPS Pt-rich γ–γ′/AM1 system after 1000 1 h-cycles at 1100 °C, each cavity located in a separate γ′ grain. Voids were also noticed by the NIMS group [35,36], after precisely 100 h at 1135 °C in a Pt-rich γ–γ′ bond-coating fabricated by Pt electroplating on the TMS-138 superalloy. When Ir was added to the coating by electroplating, the size and number of voids were much lower after a cyclic oxidation test at 1135 °C. The authors attributed this phenomenon to the lower diffusivity of Ir compared to Pt. However, it could also be due to the Ir deposition process.

Therefore, despite all these observations, the origin of void formation has not yet been proven. In the present work, the interdiffusion of a Pt coating with the Ni-13Al model alloy was investigated at 1100 °C. This enabled us to avoid the effect of alloying elements from the superalloy. Many voids were observed after interdiffusion of 1 h at 1100 °C. Moreover, to understand if the operating conditions of the electroplating process could cause the void formation, another process was considered by using SPS. A Pt foil was then interdiffused with the same substrate. This resulted in the formation of an α-phase layer. Its thickness was comparable to the Pt foil thickness. This proves that the Pt flux toward the substrate was fully compensated by the outward fluxes of Ni and Al. Therefore, no Kirkendall effect and no void appeared after 5 min at 1100 °C, consistent with the SEM observations. However, after 1 h at 1100 °C, the α phase vanished and voids were clearly present. This proves that the deposition process is not responsible for void formation, most likely due to the Kirkendall effect. Indeed, at this stage of annealing, if the inward flux of Pt is not balanced by the sum of the outward fluxes of Ni and Al, a vacancy flux is generated toward the substrate leading to a vacancy supersaturation at the Pt diffusion front. Diffusion and void formation kinetics could also be affected by the deposition process. Grain sizes in the coated layer were very different after electroplating or after SPS. Sundman et al. [25] have already pointed out that rapid initial diffusion in the Pt electroplated coating is due to the nano-sized grains. Additional numerical simulations including vacancy fluxes and grain-size effect could help to clarify the void formation and enable parametric studies in order to optimize the fabrication process.

5. Conclusion

Pt coatings were synthesized either by electroplating a 5 μm thick film or by cladding a 5 μm-thick foil by SPS on a γ-(Ni-13Al)-model alloy, followed by an interdiffusion treatment for 5 min to 10 h at 1100 °C under vacuum. The results can be summarized as follows:

1. The α-NiPtAl phase with the $L1_0$ crystal structure can form from a Pt coating on an Al-rich γ-Ni substrate. This phase formed very quickly since it was observed after a fast heating (40 °C/min) followed by 100 s dwell at 1100 °C.
2. This α phase vanishes after only 45 min–1 h at 1100 °C, with either the γ′-$(Ni,Pt)_3Al$ phase or the γ-(Ni,Pt,Al) phase formed. Based on the Ni–Pt–Al phase diagram, two diffusion paths are possible:

   (1) Pt–α-NiPtAl–γ′-$(Ni,Pt)_3Al$–γ-(Ni,Pt,Al)–Ni-13Al
   (2) Pt–α-NiPtAl–γ-(Ni,Pt,Al)–Ni-13Al.

3. Voids form at the Pt diffusion front, corresponding to the Al depletion zone, after 1 h at 1100 °C. No significant microstructural evolution is observed between 2.5 h and 10 h. Only void size and number increase with time.
4. First calculated concentration profiles in the γ-phase are promising and in reasonable agreement with those obtained experimentally.

Acknowledgments

A large part of this study was performed with the financial support of the SNECMA-SAFRAN Group. The authors would like to acknowledge Stéphane Mathieu and Michel Vilasi at Institut Jean Lamour, Nancy (France), for preparing the alloy rod, and the SNECMA-SAFRAN Group for electroplating the platinum.

References

[1] S. Bose, J. DeMasi-Marcin, J. Therm. Spray Technol. 6 (1) (1997) 99–104.
[2] K. Bouhanek, O.A. Adesanya, F.H. Stott, P. Skeldon, D.G. Lees, G.C. Wood, Mater. Sci. Forum 639 (2001) 369.
[3] B. Gleeson, W. Wang, S. Hayashi, D. Sordelet, Mater. Sci. Forum 461–464 (2004) 213–222.
[4] J.A. Haynes, B.A. Pint, Y. Zhang, I.G. Wright, Surf. Coat. Technol. 202 (2007) 730.
[5] R.T. Wu, K. Kawagishi, H. Harada, R.C. Reed, Acta Mater. 56 (2008) 3622–3629.
[6] H.M. Tawancy, A.I. Mohamed, N.M. Abbas, R.E. Jones, D.S. Rickerby, J. Mater. Sci. 38 (2003) 3797–3807.
[7] B.A. Pint, J.A. Haynes, Y. Zhang, Surf. Coat. Technol. 205 (5) (2010) 1236–1240.
[8] T. Izumi, N. Mu, L. Zhang, B. Gleeson, Surf. Coat. Technol. 202 (4–7) (2007) 628–631.
[9] R.T. Wu, X. Wang, A. Atkinson, Acta Mater. 58 (17) (2010) 5578–5585.
[10] S. Selezneff, M. Boidot, J. Hugot, D. Oquab, C. Estournès, D. Monceau, Surf. Coat. Technol. 206 (2011) 1558–1565.
[11] V.D. Divya, U. Ramamurty, A. Paul, Philos. Mag. 92 (17) (2012) 2187–2214.
[12] J.A. Haynes, Y. Zhang, W.Y. Lee, B.A. Pint, I.G. Wright, K.M. Cooley, in: J.M. Hampikian, N.B. Dahotre (Eds.), Elevated Temperature Coatings: Science and Technology III, TMS, Warrendale, PA, 1999, pp. 185–196.
[13] Y. Cadoret, D. Monceau, M. Bacos, P. Josso, V. Maurice, P. Marcus, Oxid. Met. 64 (3–4) (2005) 185–205.
[14] S. Hayashi, S.I. Ford, D.J. Young, D.J. Sordelet, M.F. Besser, B. Gleeson, Acta Mater. 53 (11) (2005) 3319–3328.
[15] D. Monceau, D. Oquab, C. Estournes, M. Boidot, S. Selezneff, Y. Thebault, Y. Cadoret, Surf. Coat. Technol. 204 (6–7) (2009) 771–778.
[16] J.L. Kamm, W.W. Milligan, Scr. Metall. Mater. 31 (11) (1994) 1461–1464.
[17] H. Meininger, M. Ellner, J. Alloys Compd. 353 (1–2) (2003) 207–212.
[18] Y. Zhang, B.A. Pint, J.A. Haynes, I.G. Wright, Surf. Coat. Technol. 200 (2005) 1259–1263.
[19] N. Vialas, D. Monceau, Surf. Coat. Technol. 201 (7) (2006) 3846–3851.
[20] A. Yamaguchi, H. Murakami, S. Kuroda, H. Imai, Mater. Trans. 48 (9) (2007) 2422–2426.
[21] Y. Zhang, J.P. Stacy, B.A. Pint, J.A. Haynes, B.T. Hazel, B.A. Nagaraj, Surf. Coat. Technol. 203 (5–7) (2008) 417–421.
[22] J.A. Haynes, B.A. Pint, Y. Zhang, I.G. Wright, Surf. Coat. Technol. 204 (2009) 816–819.
[23] J.P. Stacy, Y. Zhang, B.A. Pint, J.A. Haynes, B.T. Hazel, B.A. Nagaraj, Surf. Coat. Technol. 202 (4–7) (2007) 632–636.
[24] D. Monceau, C. Petot, G. Petotervas, Solid State Ionics 45 (3–4) (1991) 231–237.
[25] B. Sundman, S. Ford, X.G. Lu, T. Narita, D. Monceau, J. Phase Equilib. Diffus. 30 (6) (2009) 602–607.
[26] S. Hayashi, D.J. Sordelet, L.R. Walker, B. Gleeson, Mater. Trans. 49 (7) (2008) 1550–1557.
[27] S. Hayashi, W. Wang, D.J. Sordelet, B. Gleeson, Metall. Mater. Trans. 36A (7) (2005) 1769–1775.
[28] A. Vande Put, D. Oquab, D. Monceau, Mater. Sci. Forum 595–598 (2008) 213–221.
[29] B. Saint Ramond, M. Silva, J.R. Nicholls, M. Carlin, Gas turbine part provided with a protective coating, French patent 0012619 (2003), US7311981 B2, 2007.
[30] A.L. Purvis, B.M. Warnes, Surf. Coat. Technol. 133-134 (2000) 23–27.
[31] D.F. Susan, A.R. Marder, Oxid. Met. 57 (57) (2002) 159–180.
[32] Y. Zhang, D.A. Ballard, J.P. Stacy, B.A. Pint, J.A. Haynes, Surf. Coat. Technol. 201 (2006) 3857–3861.
[33] M. Boidot, S. Selezneff, D. Monceau, D. Oquab, C. Estournès, Surf. Coat. Technol. 205 (5) (2010) 1245–1249.
[34] S. Selezneff, PhD Thesis Institut National Polytechnique de Toulouse (2011)
[35] A. Suzuki, Y.N. Wu, A. Yamaguchi, H. Murakami, C.M.F. Rae, Oxid. Met. 68 (1–2) (2007) 53–64.
[36] M.C. Galetz, X. Montero, H. Murakami, Mater. Corros. 63 (10) (2012) 921–928.